ELSEVIER

Contents lists available at ScienceDirect

Journal of Environmental Management

journal homepage: www.elsevier.com/locate/jenvman



Research article

Managing a cyanobacteria harmful algae bloom "hotspot" in the Sacramento – San Joaquin Delta, California

Ellen P. Preece ^{a,b,*}, Janis Cooke ^c, Haley Plaas ^d, Alexandrea Sabo ^d, Leah Nelson ^d, Hans W. Paerl ^d

- ^a California Department of Water Resources, 3500 Industrial Blvd, West Sacramento, CA, 95691, USA
- ^b Robertson-Bryan, Inc., 3100 Zinfandel Dr., Suite 300, Rancho Cordova, CA, 95670, USA
- ^c Central Valley Regional Water Quality Control Board, 11020 Sun Center Drive, #200, Rancho Cordova, CA, 95670, USA
- d Institute of Marine Sciences, University of North Carolina at Chapel Hill, 3431 Arendell Street, Morehead, City, NC, 28557, USA

ARTICLE INFO

Handling Editor: Jason Michael Evans

Keywords: Cyanobacteria Harmful algal bloom Eutrophication Estuary Management strategies

ABSTRACT

Cyanobacterial harmful algal blooms (CHABs) have become a persistent seasonal problem in the upper San Francisco Estuary, California also known as the Sacramento-San Joaquin Delta (Delta). The Delta is comprised of a complex network of open water bodies, channels, and sloughs. The terminus of the Stockton Channel is an area identified as a CHAB "hotspot." As CHABs increase in severity, there is an urgent need to better understand CHAB drivers to identify and implement mitigation measures that can be used in an estuarine complex like the Delta. We investigated water quality conditions and nutrient dynamics in the Stockton Channel by measuring nutrients in the water column, sediments, and pore waters. In situ nutrient addition bioassay experiments were used to assess the effects of nutrient enrichment on total algal/cyanobacterial growth and pigment concentrations. In both June and September, relative to unamended controls, total chlorophyll and cyanobacterial pigment concentrations were unaffected by nutrient additions; hence, the study area showed signs of classical hypereutrophication, with ambient nitrogen and phosphorus present in excess of algal growth requirements. A cyanobacterial bloom, dominated by Microcystis spp. was present throughout the study area but was most severe and persistent at the shallowest site at the channel terminus. At this site, Microcystis spp. created water quality conditions that allowed for a prolonged bloom from June through September. While targeted nutrient reductions are recommended for long term mitigation, on a shorter timescale, our findings suggest that physical/mechanical controls are the more promising alternative approaches to reduce the severity of CHABs in the terminus of the Stockton Channel.

1. Introduction

Eutrophication is among the most pressing environmental issues impacting water resources worldwide (Likens, 1972; Smith, 2003; Sepulveda-Jauregui et al., 2018; Beaulieu et al., 2019). In estuaries, the common responses to eutrophication are increased primary productivity, changes in biogeochemical (i.e., nutrient, oxygen) cycling, and reductions in biodiversity (Glibert, 2017). Climate warming is expected to further exacerbate the symptoms of eutrophication, most notably, the increased incidences and severity of cyanobacterial harmful algal blooms (CHABs; Paerl and Huisman, 2008; 2009; Moss, 2011; Lürling et al., 2017).

River dominated coastal systems are particularly at risk of

experiencing more severe CHAB events due to the combined effects of nutrient over-enrichment, warming temperatures, and extreme weather events (Paerl, 2023). Indeed, a number of eutrophic estuaries around the world are reporting increased occurrences of CHABs (e.g., Preece et al., 2017; Paerl et al., 2018; Bargu et al., 2019). Cyanobacteria are able to proliferate in the fresh and brackish waters of estuaries, even during extreme climate variability, due to their ability to withstand large changes to water chemistry and physical properties (e.g., stratification and transparency) (Paerl and Huisman, 2008; Lehman et al., 2022).

Large estuarine systems that are prone to CHABs often have "hotspot" regions (i.e., locations where cyanobacteria blooms are most severe and most likely to occur) along the freshwater-marine continuum (Paerl et al., 2018). Mechanisms that create conditions for CHAB

^{*} Corresponding author. California Department of Water Resources, 3500 Industrial Blvd, West Sacramento, CA, 95691, USA. *E-mail address:* ellen.preece@water.ca.gov (E.P. Preece).

hotspots to develop vary by system, but can include; point sources of nutrients, flood management actions that cause freshwater pulses into an estuary, and tropical cyclones and other large storm events (Filippino et al., 2017; Vaičiūtė et al., 2021; Bargu et al., 2023). Size of the system, hydrodynamics, freshwater areas that are hydrologically isolated from high flows, and salinity gradients also influence where hotspots develop (Robson and Hamilton, 2004; Paerl, 2014; Paerl et al., 2018).

Hotspots cause transient problems as cyanobacteria cells travel from the point of origin to other portions of the watershed. This is exemplified in the St. Lucie Estuary in the southern tip of Florida's largest riverine-estuarine system, the Indian River Lagoon, that experiences severe Microcystis aeruginosa blooms that travel and accumulate from upstream Lake Okeechobee (Laureano-Rosario et al., 2021). Similar CHAB hotspot occurrences also occur in the Atchafalaya-Vermilion Bay System along the central Louisiana coast (Jaegge et al., 2023), the Klamath River in Oregon, the Yangtze River Delta in China (Liu et al., 2016; Huang et al., 2021), Himmerfjorden in Sweden (Tett et al., 2003, Walve et al., 2021), and the Curonian Lagoon in Lithuania and Russia (Vaičiūtė et al., 2021).

CHAB hotspots are also known to occur in the upper portion of the San Francisco Estuary, known as the Sacramento-San Joaquin Delta (Delta) (Spier et al., 2013; CCHAB Network, 2022). The Delta is a physically, biologically, and hydrologically complex system that receives flows from the Sacramento and San Joaquin Rivers and smaller tributaries. In addition to fluvial systems, it contains shallow flooded islands, marinas, managed canals, and static peripheral areas. The entire Delta experiences tidal fluctuations approximately twice daily. Information on CHABs in the Delta is generally limited to the flowing river regions and flooded islands (Lehman et al., 2013, 2017, 2022). Notably,

there is a paucity of studies on cyanobacteria in managed canals and static peripheral areas throughout the Delta, including the area known as the Stockton Deep Water Ship Channel (DWSC) which dead ends at the Stockton Waterfront, directly adjacent to the City of Stockton. These managed canals and static peripheral areas, including the Stockton Waterfront, are becoming recognized as CHAB hotspots (CCHAB Network, 2022; Kudela et al., 2023). Since at least 2012, CHABs dominated by the non N₂ fixing genus *Microcystis* spp. have been observed throughout the DWSC and Stockton Waterfront (Spier et al., 2013). The extent of the blooms and the associated toxin concentrations vary between years (CCHAB Network, 2022; Kudela et al., 2023). However, like other areas of the Delta, CHABs appear to have become more severe since they were first detected in the vicinity of Stockton (Lehman et al., 2017, 2022).

As CHABs have increased in intensity and frequency across the Delta, there is a pressing need to identify and implement mitigation measures. The goal of this work was to better understand nutrient dynamics and general water quality in the DWSC and Stockton Waterfront, in order to set a foundation for developing potential mitigation options. This study aimed to characterize: (i) the area within the DWSC and Stockton Waterfront with the most severe CHAB, (ii) the roles of N and P as potentially growth-limiting nutrients in the DWSC and Stockton Waterfront, (iii) identify the potential contribution of P in the sediment and pore waters to the water column, and (iv) identify potential mitigation techniques that may be appropriate to implement in a tidally influenced estuary.

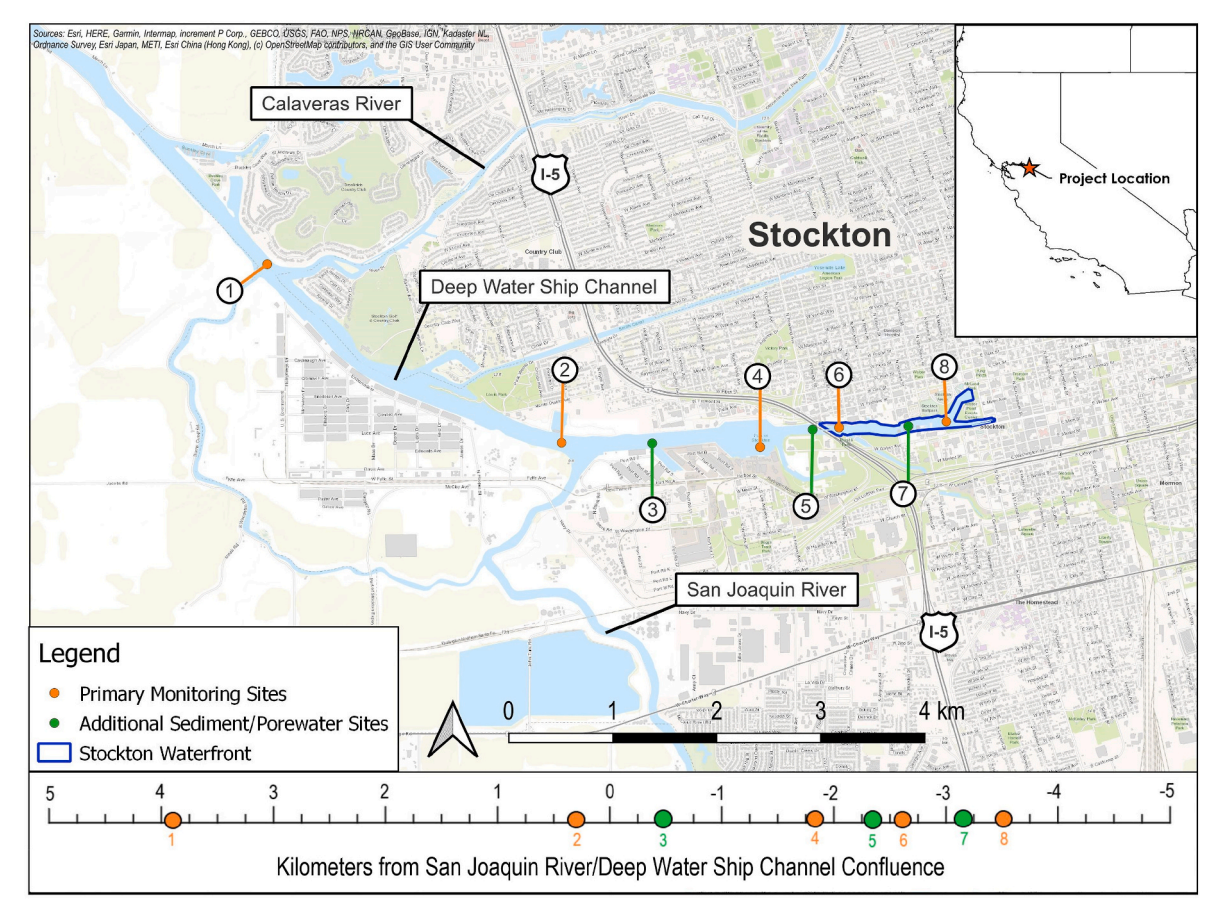


Fig. 1. Map showing the five primary sampling sites (in orange) and three additional sites where additional sediment/porewater samples were collected (in green). Sites are named as follows: 1. DWSC 4, 2. DWSC 3, 3. DWSC 2, 4. DWSC 1 (turning basin), 5. Stockton Channel Transition, 6. Waterfront 1, 7. Waterfront 2, 8. Waterfront 3. (For interpretation of the references to color in this figure legend, the reader is referred to the Web version of this article.)

2. Methods

2.1. Study site

The primary project site includes an approximately 7 km (km) long corridor through the DWSC that begins near the confluence with the Calaveras River and ends at the terminus of the channel adjacent to the City of Stockton (Fig. 1). The tidally influenced project site is approximately 150 m (m) wide and 11 m deep with the channel depth shallowing dramatically as it meets the Interstate 5 (I-5) bridge with a depth of approximately 4 m at the terminus of the channel. The DWSC is integral to the City and Port of Stockton's economy as it connects Stockton to the larger estuary and eventually the Pacific Ocean. Approximately 30 cargo vessels pass through the DWSC each month, berth in the channel, and then turn around in the turning basin.

The entire length of our study site is referred to as the Stockton Channel, but large ships only travel as far as the turning basin. We refer to the area east of the turning basin (DWSC 1) as the DWSC and the areas to the east of I-5 bridge as the Stockton Waterfront. The area between the turning basin and the Stockton Waterfront is referred to as the Stockton Channel Transition.

2.2. Field sampling

In 2022, biweekly surveys were conducted from May to November (n = 11 sampling events) at five sites along the Stockton Channel. On each date, a YSI-EXO II sonde that was calibrated following Department of Water Resources Standard Operating Procedures was used to collect data near the center of the channel at the top and bottom of the water column; temperature, dissolved oxygen, pH, specific conductivity, were recorded. An optical sensor attached to the YSI-EXO II was also used to measure total in situ chlorophyll and phycocyanin by fluorescence (Yellow Springs Instruments model 6025). In situ analysis is less accurate than laboratory extractive chlorophyll methods and cannot always pick up the signal from colonial species such as Microcystis spp. However, the sensor provides a good estimate of chlorophyll concentrations and a consistent basis of comparison between sites. Phycocyanin fluorescence sensor readings are also not well correlated with colonial species such as Microcystis spp. or in mixed species assemblages (Ma et al., 2022), but can give a general indication of cyanobacteria presence and relative changes in biomass.

A Secchi disk was used to record water clarity at each site. A *Microcystis* visual index score was also recorded at each site. Scores were ranked on a scale of 1–5, 1 meaning "absent" and 5 meaning "very high" (Flynn et al., 2022).

Water samples were collected from the surface and bottom (i.e., approximately 0.5 m above the sediment water interface) portion of the water column at each of the five primary sampling sites. Bottom samples were collected using a Kemmerer water sampler (PFTE 1.2L, Wildco Wildlife Supply Company) and surface samples were scooped with bottles by hand at approximately 0.1 m subsurface. A tow net (64 μm mesh nylon) was used to collect phytoplankton species from the surface of the water for qualitative microscopy. Samples were stored on ice during transport to the laboratories.

To estimate the concentration of sediment P and internal P cycling properties, sediment samples were collected on three dates: August 24, September 20, and November 14 (2022). The purpose of the August event was to confirm that we could successfully isolate pore waters from the samples. As such, samples for pore water analysis were only collected at the five primary sample sites. In September and November sediment samples for pore water and sediment analysis were collected from the eight sediment/porewater sites (see Fig. 1).

Sediment samples were collected using a Ponar sampler (Petite Ponar Grab Sampler, stainless steel, Wildco) to facilitate the collection of undisturbed sediment. Samplers targeted a water depth of 4–11 m to collect sediment samples. The top 5 cm of sediment was scraped off the

surface of the sediment sample, placed into glass jars, and stored on ice during transport to the laboratory.

2.3. Nutrient addition bioassay experiments

In situ nutrient addition bioassay experiments were conducted in June and September of 2022 to assess the effects of nutrient enrichment on phytoplankton growth and pigment concentrations in the Stockton Waterfront; cyanobacterial pigment concentration was approximated using the diagnostic indicator photopigments myxoxanthophyll and zeaxanthin as described in Section 2.4.2. Water was collected from Site 5 (Waterfront 1) using a submersible pump at 1 m depth and dispersed into 4 L pre-cleaned (0.01 N HCl, followed by deionized water and sample water rinses) Cubitainers (Hedwin Inc.). Cubitainers received nutrient additions in triplicate and were compared to untreated controls. In June, additions of nitrate (NO₃; KNO₃), phosphate (PO₄; KH₂PO₄), and a combined treatment of NO₃ and PO₄ were applied. In September, the same treatments were repeated with two additional treatments of NH₄ (NH₄Cl) and NH₄ and PO₄ to assess the relative growth responses to NO₃ vs. NH₄ (Table 1). Dissolved inorganic carbon (10 mg DIC; NaHCO₃) and silica (43.75 μM; SiO₂) were also added to each Cubitainer to ensure these nutrients were not depleted during the bioassay period. Following nutrient additions, samples were suspended in a floating corral fitted with a layer of neutral density screening (to prevent photooxidation) off a dock in the San Joaquin River in Antioch, CA, to incubate at ambient light and temperature conditions for six continuous days. On experiment days 1 (T0), 2 (T1), 4 (T2), and 6 (T3), subsamples were taken from each Cubitainer and processed for chemical analyses, including dissolved nutrients, chlorophyll a, diagnostic group-specific phytoplankton chlorophyll and cartenoid pigments and particulate carbon and nitrogen (CHN).

2.4. Laboratory analyses

2.4.1. Water column samples

Upon sample receipt, 10 mL (mL) aliquots of each surface and bottom water sample were collected into 15 mL pre-cleaned Falcon tubes and stored at -20 °C until processing; these samples were analyzed for total nitrogen (TN) and total phosphorus (TP). Similarly, 10 mL of each sample were syringe-filtered (0.7 μm pore size) and stored at $-20\ ^{\circ}C$ until further processing; these samples were analyzed for dissolved nutrients (i.e., PO₄, NO₃, and ammonia - NH₃). Nutrient concentrations were analyzed following standard procedures and using Hach TNT plus chemistries (Hach Methods 10,205, 10,206, 10,208, 10,209, and 10,210). Positive and negative controls consisted of Hach Mixed Parameter Standard (LCA 721) and laboratory deionized water, respectively. All reaction vials were read using a Hach DR3900 spectrophotometer with associated reagents in accordance with established EPA methods or surrogate methods (Nitrate Method 10,206, Ammonia Nitrogen Method 10,205, Total Nitrogen Method 10,208, Total and Reactive Phosphorus Method 10,209/10,210).

2.4.2. Bioassay samples

Photopigment concentrations diagnostic for major phytoplankton groups were determined using high-performance liquid chromatography (HPLC) (Shimadzu model LC-20AB) equipped with an autoinjector (SIL-20AC) and photodiode array spectrophotometric detector (Shimadzu SPD-M20A). This is an important distinction since all chlorophyll/pigment concentrations collected in the field were estimated using an *in situ* YSI sonde (fluorescence), but chlorophyll/pigment concentrations collected during the bioassay experiments were quantified using HPLC (ug/L, absorbance).

Phytoplankton groups included chlorophytes (chlorophyll *b*), cyanobacteria (zeaxanthin and myxoxanthophyll), diatoms (fucoxanthin), dinoflagellates (peridinin), and cryptophytes (alloxanthin) (Jeffrey et al., 1999). Total phytoplankton pigment concentration was

Table 1

Nutrient additions for each treatment of the bioassays in June and September. Values were selected to mimic typical summertime concentrations in the Stockton Waterfront using ambient nutrient concentrations from monitoring data accessed through the United States Geological Survey's online portal (Bergamaschi et al., 2020).

Bioassay		Treatments	Treatments							
Month	Nutrient	Control	NO3 (KNO3)	P (KH2PO4)	NO3 (KNO3) + P (KH2PO4)	NH4 (NH4Cl)	NH4 (NH4Cl) + P (KH2PO4)			
June	N	_	87.5 μM N	_	87.5 μM N	_	_			
	P	_	_	17.5 μM P	17.5 μM P	_	_			
Sept	N	_	87.5 μM N	_	87.5 μM N	87.5 μM NH	87.5 μM NH			
	P	_	_	17.5 μM P	17.5 μM P	_	17.5 μM P			

determined by adding these pigment concentrations together and chlorophyll *a* concentration, also determined via HPLC, was used as a proxy for total pigment concentration for statistical analyses. Soluble nutrient concentrations were determined with a LACHAT QuikChem 8000 Flow Injection Analysis System utilizing LACHAT Instruments' QuikChem methods for total dissolved nitrogen (TDN) (Method 10-107-04-3-P) and a SEAL QuAAtro39 Continuous Segmented Flow Analyzer (QuAAtro SEAL Analytical Inc.) following SEAL method guidelines in accordance with standard U.S. EPA methods for PO4 (Method no. Q-037-05 Rev. 4), NH4 (Method no. Q-033-04 Rev. 8), and NO3 (Method no. MT3B Q-035-04 Rev 10).

2.4.3. Sediment and pore water samples

To evaluate the potential for internal P cycling, we analyzed sediment and pore water from eight sites. Sediments were analyzed for grain size and total organic carbon. Grain size was measured using variable sieve sizes to isolate fractions (PSEP, 1997). A triplicate analysis of one sample was analyzed per batch. All triplicate analysis has a coefficient of variation less than 5%. Organic carbon was analyzed by non-dispersive infrared spectroscopy (Method SW846 9060A; AOAC, 1997; Harris et al., 2001). Sediments were dried at 70 °C and acidified and purged with nitrogen to remove inorganic carbon prior to oxidation by combustion.

To extract pore water, 6 g of wet sediment was weighed and placed into 50 mL polypropylene centrifuge tubes. Samples were spun at 4000 rpm for 20 min on a Fristaden Lab benchtop centrifuge. Pore water was decanted then filtered through Whatman borosilicate glass microfiber GF/D filters (2.7 μ m pore size) into fresh centrifuge tubes prior to analysis. TP was measured in the filtered pore water samples following the same methods as described above for water column nutrient analyses.

2.5. Data analysis

Correlations between samples collected at the top and bottom of the water column were tested using Pearson's correlation with statistical significances at the p <0.05 level (one-tailed). Positive correlations were used to determine if the top and bottom water column samples were correlated and could be treated as a single variable for further data analysis.

Principal component analysis (PCA) was employed to compare patterns between water quality data and to visualize differences in water quality across the five primary sampling sites. Eigenvalues greater than 1 were considered as the criterion for the extraction of the principal components to elucidate the variances found in the data. To verify the PCA results and test the significance of clustering between sites, a PERMANOVA based on Euclidean distance matrices was performed with 999 permutations. A pairwise comparison using Euclidean distance and the Holm correction was used to determine significant differences between sites.

Differences in mean water quality variables was analyzed using oneway ANOVA tests. A post hoc multiple means comparison test with 95% confidence intervals was used to compare mean water quality variables across sites via specific linear combinations by the Tukey method. In order to evaluate differential cyanobacterial growth and overall pigment concentration between nutrient addition treatments of the bioassay experiment, the following statistical analyses were performed. Cyanobacterial indicating pigments and total chlorophyll a (measured via HPLC, as a proxy for total pigment concentration) concentrations for each treatment were compared to the control on T3 (experiment day 6) using a two-way ANOVA test (a =0.05). A post hoc multiple means comparison test with 95% confidence intervals was used to compare each nutrient treatment to one another (e.g., NH4 to NO3) via specific linear combinations by the Tukey method.

Differences in TP concentrations between the water column and pore water were tested with t-tests. A one-way ANOVA was used to test if there were differences in TP pore water concentrations across sites.

Statistics and visualizations were completed in R v.7.2 (http://cloud. r-project.org) using the 'factoextra', 'vegan', and 'ggplot' packages (Oksanen et al., 2022).

3. Results

3.1. Water quality conditions

Water quality differed among sites, with surface water quality conditions during the primary bloom season (defined as June through September) characterized by high mean water temperatures (25.0–26.3 °C), pH (7.8–9.5), and daytime dissolved oxygen concentrations (6.9–12.5 mg/L) (Table 2). Mean specific conductivity was relatively low at all sites (491–566 μ S/cm) but was highest at the DWSC sites and then decreased in an eastward direction as expected with the estuarine gradient. The Waterfront 3 site had the highest maximum temperature, maximum dissolved oxygen, and maximum pH, lowest maximum specific conductivity, and densest cyanobacteria bloom of all sites. The Waterfront 3 site had significantly higher mean dissolved oxygen, pH, chlorophyll, *Microcystis* visual index, and lower secchi depth than the sites in the Deep Water Ship Channel (p < 0.05). The bloom at the Waterfront 3 site also lasted the longest, with *Microcystis* spp. colonies still present on the last sampling date in November.

From June through October, *Microcystis* was the dominant genus observed at all study sites. Other genera that were present included cyanobacteria *Planktothrix*, *Aphanizomenon*, *Dolichospermum*, *Pseudanabaena*, as well as numerous chlorophyta, and diatom genera.

The Pearson's correlation analysis of water samples collected from the top and bottom of the water column showed significant positive correlations for all nutrient forms and other water quality parameters (Fig. 2). The strong positive correlations between the top and the bottom of the water column indicated that samples could be treated as a single factor for further analysis. Although most factors were positively correlated, NH_3 –N was negatively correlated with temperature, dissolved oxygen, pH, chlorophyll, phycocyanin, TN, TP, and PO_4 .

Importantly, the PCA revealed some distinct traits of the DWSC: firstly, that key indicators of cyanobacterial blooms (visual index scores, chlorophyll, etc.) were not strongly correlated with dissolved nutrient concentrations or temperature. The first two principal components accounted for the majority of variance (64.9%) (Fig. 3). Principal component 1 showed that NH3–N and Secchi depth had an inverse

Table 2 Maximum water depth and mean \pm standard deviation of surface water quality variable (except for pH which is reported as the median) measured twice per month at the five primary stations between June 13 and September 30, 2022 (n = 8). Maximum recorded value presented in parentheses. Different letters indicate statistically significant differences between sites (p < 0.05).

Site	DWSC 4	DWSC 3	DWSC 1	Waterfront 1	Waterfront 3
Water Depth, m	12	11	12	6	4
Water Temperature, °C	25.0 ± 1.3 (26.8), A	25.1 ± 1.3 (26.9), A	25.5 ± 1.3 (27.5), A	25.8 ± 1.3 (27.6), A	26.3 ± 1.3 (28.3), A
Percent Dissolved Oxygen, %	81 ± 7 (90), A	76 ± 7 (90), A	94 ± 22 (136), A	102 ± 18 (122), A	148 ± 42 (203), B
Dissolved Oxygen, mg/L	6.7 ± 0.5 (7.5), A	6.3 ± 0.6 (7.5), A	7.6 ± 1.8 (11.3). A	8.3 ± 1.4 (10.1), A	11.8 ± 2.9 (15.2), B
Specific Conductance, μS/cm	608 ± 155 (853), A	586 ± 182 (821). A	592 ± 204 (858), A	582 ± 190 (827), A	562 ± 165 (807), A
pH	7.8 ± 0.1 (8.0), A	7.7 ± 0.1 (7.8), A	7.9 ± 0.7 (9.8), A, B	8.6 ± 0.6 (9.6), B, C	9.5 ± 0.6 (9.8), C
Chlorophyll fluorescence, mg/L	1.6 ± 0.61 (2.9), A	1.6 ± 0.6 (2.5), A	5.0 ± 2.6 (10.1) A,B	8.4 \pm 4.1 (13.9) B,C	12.4 ± 3.8 (16.1), C
Microcystis Visual Index	2.0 ± 0.5 (3.0) A	1.9 ± 0.4 (2.5) A	2.8 ± 0.6 (3.5) A,B	3.5 ± 0.6 (4.5) B	4.4 ± 0.5 (5), C
Secchi Disk, m	5.5 ± 1.2 (7.0) A	$4.8 \pm 0.7 \ (5.8) \ A$	4.5 ± 0.8 (5.5) A	3.6 ± 0.9 (5.3) A,B	2.3 ± 0.8 (3.5) B
Total Phosphorus (TP) mg/L	$0. \pm 0.04$ (0.44), A	0.45 ± 0.06 (0.55), A	0.43 ± 0.06 (0.53), A	0.43 ± 0.05 (0.52), A	0.52 ± 0.20 (0.97), A
Phosphate (PO ₄) mg/L	0.34 ± 0.05 (0.40), A	0.42 ± 0.09 (0.56), A	0.39 ± 0.06 (0.46), A	0.38 ± 0.08 (0.49), A	0.35 ± 0.11 (0.48), A
Total Nitrogen (TN) mg/L	2.34 ± 0.63 (3.04), A	2.79 ± 0.77 (4.33), A	2.78 ± 0.60 (3.69), A	2.75 ± 1.02 (4.75), A	2.82 ± 1.70 (6.44), A
Ammonia (NH ₃) mg/L	0.05 ± 0.03 (0.10), A, B	0.10 ± 0.03 (0.17), A	0.06 ± 0.03 (0.13), A, B	0.04 ± 0.04 (0.12), B	$0.03 \pm 0.05 \ (0.14), B$
Nitrate (NO ₃) mg/L	$1.71 \pm 0.65 \ (2.63), A, B$	2.14 ± 1.00 (4.38), A	2.06 ± 0.76 (3.62), A, B	1.74 ± 0.56 (2.93) A, B	$0.96 \pm 0.51 \ (2.07), B$

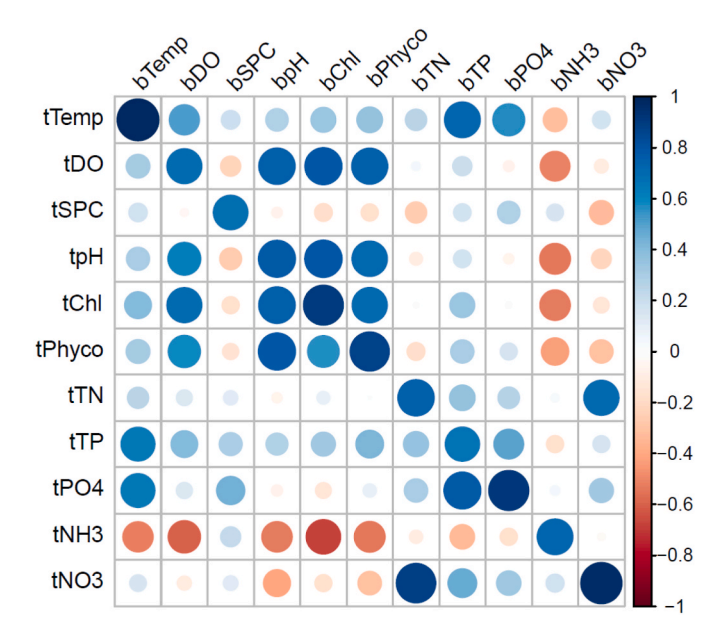


Fig. 2. Correlation matrix showing correlation between samples collected from the top (t) and bottom (b) of the water column from the five primary sample sites. Blank cells show no significant correlation between variables (p > 0.05). Blue circles indicate a positive correlation between variables while red circles indicate a negative correlation between variables. The darker and larger the circle the more significant the correlation. (For interpretation of the references to color in this figure legend, the reader is referred to the Web version of this article.)

relationship with pH, dissolved oxygen, chlorophyll, phycocyanin, and the visual index. These findings indicate that NH_3 –N and water clarity decrease as cyanobacteria biomass increases. However, temperature and the dissolved nutrients (other than NH3–N) were more explained by principal component 2 (Fig. 3). These factors are likely less associated with the main bloom indicators because nutrients are present in excess throughout the entire study area (Fig. 4).

The PCA also revealed that the sites sampled along the Stockton Channel are ecologically distinct. To demonstrate statistically significant differences between the primary sampling sites, colors were assigned to each of the five sites and 95% confidence ellipses are drawn around clusters identified by the PCA calculations. These ellipses indicate that sites are divided into three groups: on the left are the two sites in the main portion of the DWSC. These sites had much lower concentrations of cyanobacteria as indicated by visual index data, chlorophyll, and phycocyanin than the other groups. In the middle, straddling the left

and right are the DWSC 1 and Waterfront 1 sites (Fig. 3). These are part of the transition zone of the Stockton Channel and are characterized as having higher visual index scores, chlorophyll, and phycocyanin than the DWSC sites, but lower amounts of cyanobacteria than Waterfront 3. Finally, Waterfront 3 was primarily on the right side of the PCA plot. This site consistently had the highest visual index scores, and the highest concentrations of chlorophyll and phycocyanin of all the study sites. A PERMANOVA test confirmed significant differences between the PCA ellipses (p < 0.001). Pairwise comparisons show that the Waterfront 3 site was significantly different than the other four primary sampling sites: Waterfront 1 (p = 0.023), DWSC 1 (p = 0.002), DWSC 3 (p = 0.001), and DWSC 4 (p = 0.001). Waterfront 1 was significantly different from DWSC 3 (p = 0.004) and DWSC 4 (p = 0.17). Pairwise comparisons did not reveal significant differences between the other sites.

3.2. Nutrients in the water column

Nutrient concentrations in top and bottom samples for each site are plotted on the same figure (Fig. 4). TP and PO_4 concentrations consistently exceeded the threshold for nutrient limitation of (0.1 mg/L) and (0.01 mg/L) respectively (Ibelings et al., 2021), but the exact TN-threshold concentrations were less clear. A review by Ibelings et al. (2021) suggests that TN concentrations above which N-limitation of phytoplankton biomass becomes unlikely is somewhere in the range of 0.35–2 mg/L.

The minimum TN measured was 1.18 mg/L in November at the Waterfront 3 site. Overall, TN was lowest at all sites during the October and November sampling dates. From May to September, TN was generally high and exceeded the proposed 2 mg/L TN threshold concentration below which N is likely to limit further phytoplankton biomass (Ibelings et al., 2021). NH₃–N was consistently lowest at the Waterfront 3 site where chlorophyll concentrations were highest. NO_3 –N appeared to decrease with highest concentrations measured at the beginning of the sampling period in May and lowest concentrations measured at the end of the sampling period in October and November.

3.3. Effects of nutrient enrichment on cyanobacterial pigment concentrations

In June, phytoplankton communities were composed of a mixed assemblage of chlorophytes, cryptophytes, and cyanobacteria in relatively equal concentrations, but in September, diatoms dominated, followed by chlorophytes then cyanobacteria. Cryptophyte pigment concentrations remained low and dinoflagellate pigments were not observed during both experiments. Per the concerns associated with cyanobacterial blooms in the study area, the main focus of nutrient

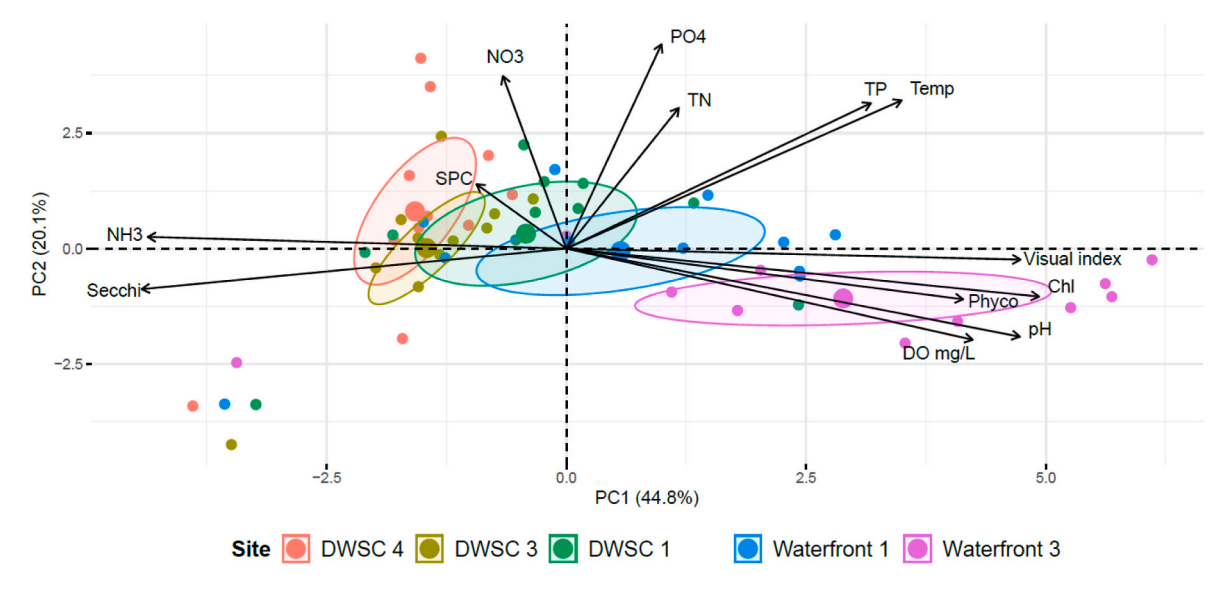


Fig. 3. Principal component biplot for the first two principal components. The arrows originating from the central point of the PCA biplot indicate positive or negative correlations of different variables. The closeness of arrows indicates correlation strength between variables. To facilitate visual identification of patterns, 95% confidence ellipses were constructed around clusters for each of the five primary sampling sites.

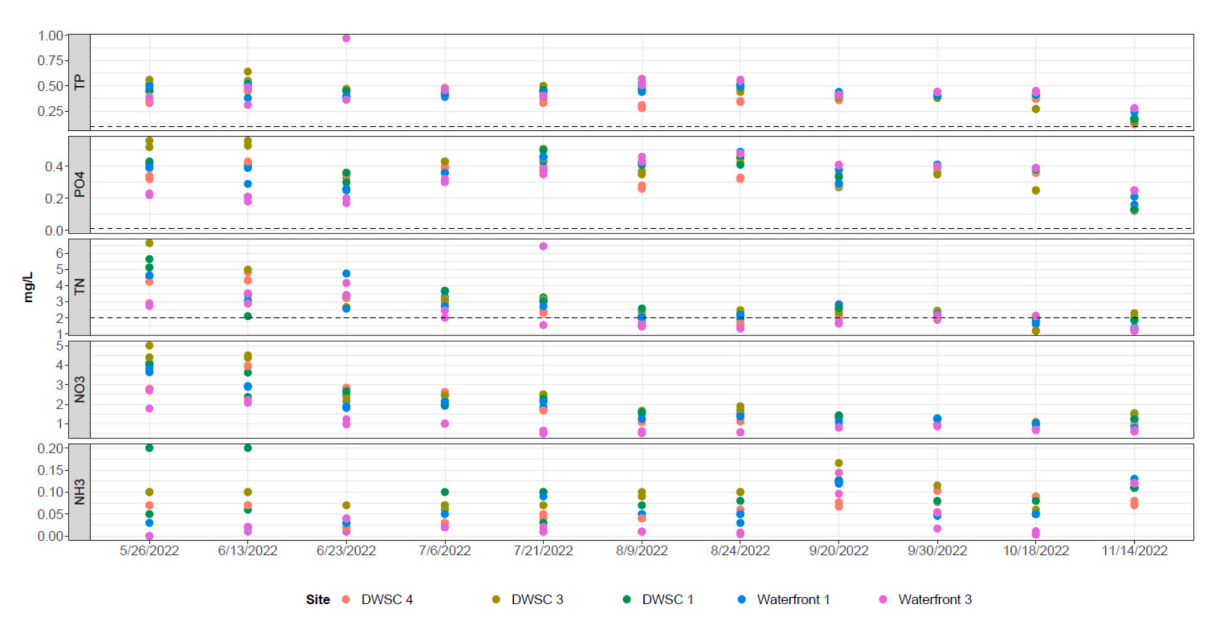


Fig. 4. Total phosphorus (TP), orthophosphorus (PO_4), total nitrogen (TN), nitrate (PO_3 -N), and ammonia (PO_4 -N) plotted by date for each of the five primary sampling sites. Top and bottom water column samples are shown on the same plot so there are two samples plotted per date, per site. The black dotted lines are nutrient thresholds that are cited in the literature as limiting cyanobacteria growth (Ibelings et al., 2021). Each point represents a single sample.

addition experiments was on the stimulation of cyanobacteria. Accordingly, for the primary analysis, chlorophyte, diatom, dinoflagellate, and cryptophyte pigment concentrations were grouped for direct comparison to cyanobacterial pigments (derived from diagnostic pigment analysis as described in Section 2.4.2) (Fig. 5).

As demonstrated in the control group responses, final cyanobacterial pigment concentrations in Waterfront 1 were greater during the June bioassay (20.09 \pm 0.55 µg/L at T3) when compared to September (1.11 \pm 0.12 µg/L at T3) (Fig. 5), as expected by the seasonal and temperature preferences of the blooms (Lehman et al., 2017). During the June bioassay, in the absence of any N or P nutrient additions (control group), cyanobacterial pigment concentrations rose by more than 8 times over the course of the 6 day experiment with the largest growth occurring between T2 and T3 (Fig. 5). Similarly, HPLC-determined chlorophyll a in all treatments more than tripled by T3. In a stark difference, during

the September experiment, cyanobacterial pigment concentration less than doubled (Fig. 5), but HPLC-determined chlorophyll a concentrations still increased considerably, beginning at 7.66 \pm 0.21 on T0 and ending at 70.52 \pm 1.24 µg/L on T3. This suggests that cyanobacterial communities outcompeted many of the other algal groups in June, but they did not in September when they contributed to a much smaller fraction of total chlorophyll a. However, it is important to note that all observed growth dynamics were consistent between controls and nutrient treatments (adj. p > 0.05) in both months. During both experiments, there were no statistically significant differences in chlorophyll a observed between all treatments at T3, with the exception of NO3 vs NO3+P in June (adj. p < 0.05). These findings indicate that nutrient concentrations present in the original water samples were already in excess of phytoplankton growth needs and that the nutrient additions failed to stimulate further growth.

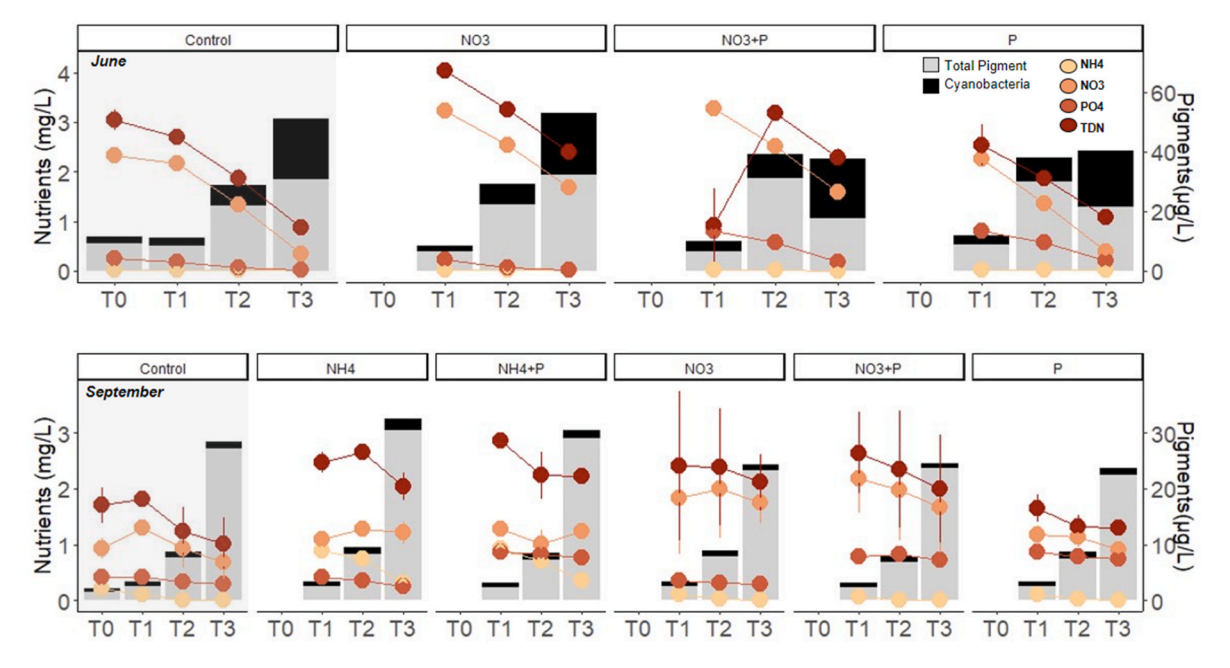


Fig. 5. Total phytoplankton pigment concentrations and nutrient concentrations recorded during the June and September 2022 bioassay experiments. Phytoplankton concentrations is reported on the right y-axis in μ g/L, nutrient concentrations are reported in mg/L on the left y-axis. Note the difference in y-axes scales in June vs. September. Pigments indicating cyanobacteria (myxoxanthophyll and zeaxanthin) are shown in black, and all other detected pigments (alloxanthin (cryptophytes), chlorophyll b (chlorophytes), and fucoxanthin (diatoms)) are visible in gray.

Nutrient concentrations exceeding the needs of cyanobacterial communities were confirmed by the high concentrations of TDN, NO3, NH4, and PO4 measured during the experiments. Total dissolved nitrogen (TDN) was 3.04 ± 0.21 mg/L in June and 1.70 ± 0.32 mg/L in September at T0, continuously exceeding nutrient thresholds of 1.00-1.30 mg/L reported as limiting cyanobacterial growth throughout the summer months (Ibelings et al., 2021). In June, by T3 of the experiment, only two-thirds of the TDN available had been used up in the control, leaving ample N left to support growth. Similarly, in September, less than one-half of the total available TDN at T0 was depleted by the control group.

3.4. Pore waters and sediments

Sediment at the sites was generally dominated by silt, clay, and sands with less than 30%, by mass, of grain composed of gravel (Fig. 6). The exception to this was the Waterfront 1 site where over 50% of the sediment was composed of gravel. Waterfront 3 and Stockton Channel Transition also had higher gravel content than the other sites.

Sediment organic carbon content was higher in the shallower portions of the Stockton Channel, with the highest organic carbon at Waterfront 3 (Table 3). At Waterfront 3 organic carbon content in the sediments was almost five times higher than the DWSC sites. Grain size did not appear to influence organic carbon content.

Pore waters were variable across sites and dates (Table 3). Pore

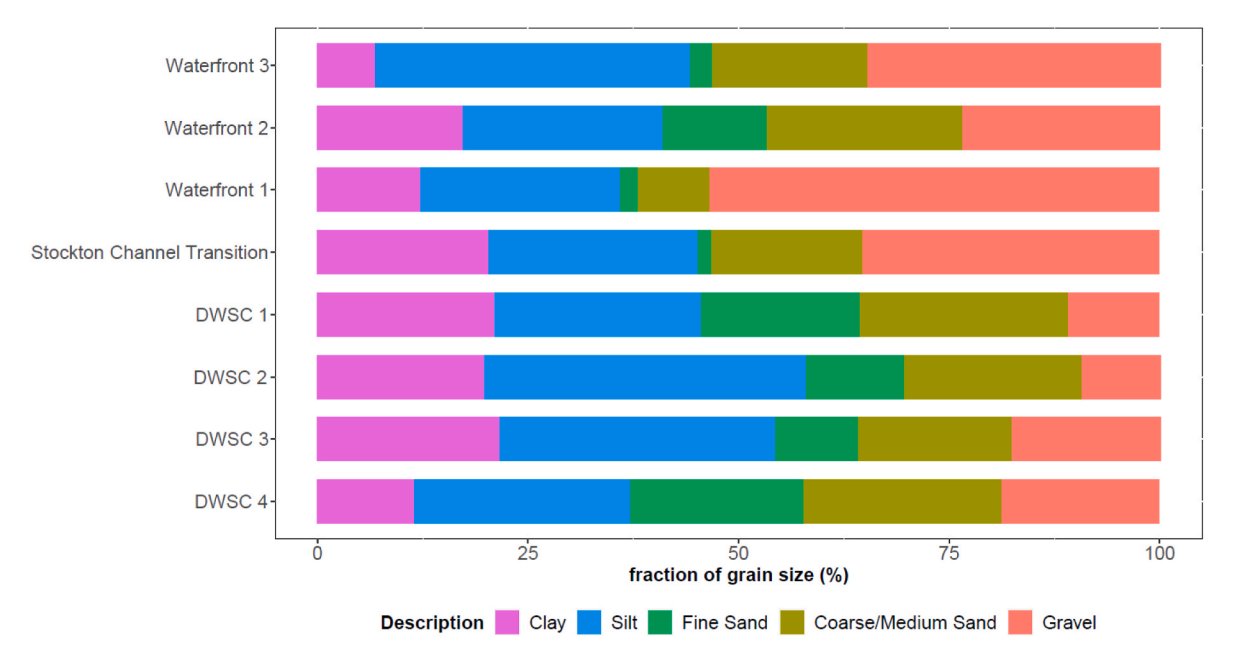


Fig. 6. Percent grain size measured at each of sediment sampling sites by mass.

Table 3

Total phosphorus (TP) in pore waters from August September and November 2022. TP and organic carbon in sediments collected in September and November 2022. Each value represents a single sample.

Site	Organic Carbon in mg/kg (dry weight)		TP in sediment mg/kg		Total Filterable P in pore waters mg/L		
	September	November	September	November	August	September	November
Waterfront 3	276,000	247,000	430	310	1.2	0.4	0.6
Waterfront 2	178,000	_	540	790	-	0.8	0.3
Waterfront 1	164,000	_	380	340	0.7	0.6	0.5
Stockton Channel Transition	165,000	140,000	540	320	-	0.5	0.7
DWSC 1	51,600	74,600	410	510	0.9	1.4	1.2
DWSC 2	65,100		460	380	_	0.2	0.9
DWSC 3	61,500	_	460	390	0.6	1	0.4
DWSC 4	54,900	37,100	300	87	0.6	0.3	0.9

waters had consistently higher total filterable P concentrations than TP in the overlying water column (Fig. 7) Welches t-test confirmed a significant difference between total filterable P in pore water and TP in the overlying water column (p < 0.001).

TP in the surface sediments generally ranged from 300 to 540 mg/kg (Table 3). However, there were two outliers in November; one sample at the DWSC 3 was 87 mg/kg while one sample collected at the Stockton Channel Transition contained 790 mg/kg of TP.

4. Discussion

As previously reported and confirmed here, a *Microcystis* spp. bloom occurred in the Stockton Channel throughout the summer of 2022 (Spier et al., 2013; CCHAB Network, 2022). Although other species of cyanobacteria were also present intermittently, *Microcystis* spp. dominated at all sites from late June through September. In addition to non-limiting nutrient concentrations, the study area exhibited warm water temperatures throughout the summer season with mean water temperatures at or above 25 °C.

The study area showed signs of classical hypereutrophication, with N and P available in non-limiting amounts (Ibelings et al., 2021). Bioassays confirm hypereutrophic conditions, both due to the lack of N or P (or N + P) stimulation by additions and the high ambient N and P concentrations measured in the controls throughout the bioassay period. Interestingly, per amount of N, experimental additions of NH₄ slightly stimulated phytoplankton production more than NO₃. This supports previous work, showing a preference for reduced forms of N, especially among cyanobacteria (Blomqvist et al., 1994; Lehman et al., 2017; Newell et al., 2019). On most dates, Waterfront 3 had lower NH₃ compared to the other sites, possibly because it was marginally limiting

as suggested by the nutrient addition experiments.

The Delta has become well recognized for having nutrient conditions that can exceed phytoplankton growth requirements (e.g., Wilkerson et al., 2006; Lehman et al., 2015; Frantzich et al., 2018). However, nutrient concentrations in the Stockton Channel were notably high even for the Delta (Lehman et al. 2017, 2022). High nutrient concentrations in the Delta have been tied to a combination of point and non-point sources (Jassby, 2008, Saleh and Domagalski, 2021). In the Stockton Channel there is also a large nutrient pool stored in the sediments and pore waters that likely contributes nutrients to the water column. These findings are consistent with Cornwell et al. (2014) who found significant and dynamic sediment nutrient fluxes especially in shallower areas of the Delta. There were indications of internal P loading across all sites due to the high concentrations of P in the pore waters, but flux rates of phosphorus from sediment were not quantified in this study. Further study is necessary to determine if the observed differences in sediment size and composition influenced internal nutrient loading in the study area (Wang and Li, 2010; Gao et al., 2014, Rahutomo et al., 2018).

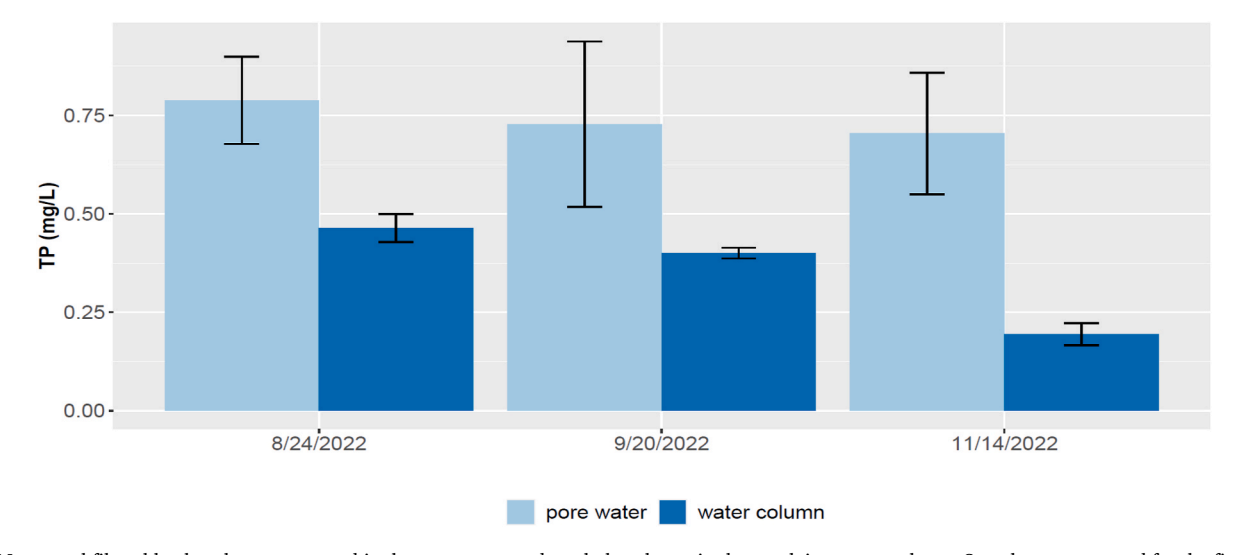


Fig. 7. Mean total filterable phosphorus measured in the pore water and total phosphorus in the overlying water column. Samples are averaged for the five primary sampling sites, on each date, where pore water was collected. Black bars show standard error.

than the pH at all the other sites which was likely driven by the high amount of *Microcystis*. This observation aligns with other studies that have found *Microcystis* not only grows well at high pH, but it also adapted to utilize bicarbonate as a carbon source and in doing so drives pH even higher during photosynthesis (e.g., Sandrini et al., 2016; Visser et al., 2016; Zepernick et al., 2021). Along the Stockton Waterfront sediment organic carbon was 4–5 times higher than the DWSC sites. Considering these factors, the large bloom at Waterfront 3 likely generated a positive feedback loop to sustain the bloom by keeping pH high and increasing deposition of organic matter into the sediment, which can promote internal nutrient cycling (Gao et al., 2014, Qin et al., 2020). Internal and external nutrient loading likely created favorable conditions that allowed for a sustained *Microcystis* spp. bloom.

This study did not evaluate hydrodynamics of the study area, but the Waterfront 3 site is demonstrated to be lacustrine in nature (Schladow and Monismith, 2009), and these characteristics likely also impact the development and sustained presence of *Microcystis* spp. at this site. Factors such as the channel morphology, depth, and different hydrodynamic conditions likely contributed to the less severe bloom in the DWSC. These physical differences have been identified as factors limiting cyanobacteria growth, accumulation and/or bloom crashes in other CHAB hotspots where nutrients are replete (Qin et al., 2020, Wang and Zhang, 2020).

4.1. Implications for controlling cyanobacteria blooms

Managing CHABs has become increasingly complicated, especially as blooms have expanded across the freshwater to marine continuum (Zepernick et al., 2023). As such, there is no one size-fits-all management approach for any given water body (Erratt et al., 2022). In our study area it is clear that CHABs are most severe at the Waterfront 3 site and we suggest that initial mitigation efforts should focus on this area of the Stockton Channel. It is possible that mitigating this CHAB hotspot may also reduce cyanobacteria biomass downstream in the DWSC (Phlips et al., 2023).

CHAB management tools that could be used in estuaries can be divided into four main categories: 1) external nutrient control that addresses point and non-point sources, 2) chemical controls in the form of algaecides or barley straw to control blooms or flocculants to control internal nutrient loading, 3) biological controls that alter the physiology of cells, introduce top-down biological control agents, or macrophytes to compete with cyanobacteria, and 4) physical/mechanical controls to increase flushing and reduce retention time, hydrologic modifications that can circulate water sufficiently to disrupt the life history strategy of buoyant cyanobacteria and prevent the accumulation of colonies, or dredging that removes nutrients and cyanobacteria seedstock (Paerl et al., 2018; Kibuye et al., 2021a, 2021b). Based on our study results, and considering the physical, ecological, and management complexity of the Delta, we narrow the possible mitigation options that are realistic for the Stockton Waterfront below.

In theory, managing eutrophication itself is straightforward – reduce excess nutrient supply (Paerl, 2014). Yet, in practice managing nutrient supply in a large hydrologically complex estuary is exceedingly difficult (Dolph et al., 2017). Given that nutrient levels in the water column and sediments in the study area are elevated, reductions in nutrient inputs from a few specific sources (e.g., point source, stormwater) are unlikely to rapidly improve water quality conditions in the Stockton Channel (Xu et al., 2021). Further, it is not feasible in the short-term to achieve these point source reductions as regulations to achieve decreases in nutrient point sources would take a number of years to implement. Nevertheless, in the long-term, nutrient reductions at a watershed scale may be needed to decrease occurrences of cyanobacteria in the area.

Chemical and biological controls are currently not realistic near-term options for managing water quality, preventing cyanobacteria blooms, or suppressing established blooms in the Delta. This is because of the cost, application challenges, lack of research and testing for biological

and chemical controls in a tidal environment, presence of federally and state listed special status fish species, and a complex regulatory and institutional structure with a multi-step process for obtaining appropriate permits and approvals (Luoma et al., 2015; Ta et al., 2017). It is also notable that chemical control techniques for other primary producers in the Delta have at best, ephemeral success likely because these techniques are intended for use in lentic systems that do not experience tidal fluctuations (Larsen et al., 2023). Use of biological controls such as macrophytes are unlikely to get approval as managers are struggling to control the invasive macrophytes that are currently invading many areas of the Delta (Ta et al., 2017).

Increasing streamflow has been shown to inhibit CHAB development in the Neuse River estuary, North Carolina, USA, and Scheldt Estuary, The Netherlands (Christian et al., 1986; Verspagen, 2006; Yang et al., 2018). Yet in the Delta, there have long been issues reconciling and balancing competing objectives and resource demands related to water supply (Lund, 2016). These issues have been exacerbated over the past decade as drought has affected the reliability of the regional water supply (Alexander et al., 2018). Further, the Waterfront is isolated from the major rivers that control streamflow through the Delta. The nearest major river to the Waterfront, the San Joaquin River, is over 2.5 km downstream from the western edge of the Waterfront and over 3.5 km from Waterfront 3 where the most severe blooms form.

In the near-term, the evaluation of mitigation measures could focus on physical/mechanical controls along the Stockton Waterfront to reduce the occurrence and severity of cyanobacteria blooms in the area. There are some physical controls currently in place to alleviate the problems associated with low dissolved oxygen concentration but were not intended to decrease CHABs. There are two aeration facilities owned by the Port of Stockton that add approximately 8500 pounds of pure gaseous oxygen into the water of the DWSC to maintain dissolved oxygen concentrations at or above water quality objectives. The aeration facilities are turned on when needed, typically late summer for 2-10 days at a time. Fixed station and boat-mounted DO measurements, hydrodynamic modeling and dye studies indicate the effects of the aerators are extensive but likely do not measurably affect DWSC 1 or the Waterfront sites. Along the Stockton Waterfront there are nine line diffuser bubbler systems that are spaced every 500 feet on the floor of the channel from just west of Waterfront 1 to the eastern terminus of the channel. During our study, the line diffuser bubbler system appeared to have little, if any, impact on the formation of CHABs in the area as dense Microcystis scum formed directly over the bubblers. The system likely does not create enough turbulence and mixing of the water column to reduce Microcystis biomass production (Huisman et al., 2004).

Increasing the physical recirculation of the water throughout the Waterfront, but with a focus on the Waterfront 3 site, is a promising near-term option for managing CHABs in the area. To supplement physical recirculation, it may be useful to remove or reduce organic carbon, nutrients, and overwintering *Microcystis* seedstock through dredging. Combining dredging with other mitigation methods has been effective at improving water quality in other estuarine systems (Chen et al., 2021).

5. Conclusions

We present several independent lines of evidence for hypereutrophic conditions in the Stockton Channel throughout the cyanobacterial growth season. However, nutrients alone do not explain why blooms were so severe at the terminus of the channel. Blooms may be most severe at Waterfront 3 because it is shallowest, warmest, and most lacustrine site. Dense cyanobacterial blooms may drive a positive feedback cycle by increasing and maintaining high pH, affecting dissolved oxygen concentrations, and creating high amounts of organic carbon in the sediment to continue fueling the bloom. Considering study results and the ecological, physical, and institutional complexity of the Delta, physical/mechanical mitigation measures appear to be the

promising option for managing blooms at the Waterfront. In the long term external nutrient reductions will also likely be necessary to mitigate the blooms. Findings from this study are relevant for considering mitigation actions in other "hotspots" of the Delta as well as other estuaries that experience CHAB hotspots.

Credit author statement

Ellen P. Preece: Conceptualization, Investigation, Formal analysis, Writing – original draft, Visualization, Funding acquisition, Project administration: Janis Cooke Conceptualization, Investigation, Resources, writing-reviewing and editing, Funding acquisition Haley Plaas: Conceptualization, Investigation, Writing – original draft, Visualization, Formal analysis. Alex Sabo: Formal analysis, Visualization, Writing – original draft, Data Curation Leah Nelson: Investigation, Writing- original Draft, Visualization, Formal Analysis. : Hans Pearl: Supervision, Resources, Funding acquisition, Writing-reviewing and editing, Project administration

Declaration of competing interest

The authors declare the following financial interests/personal relationships which may be considered as potential competing interests: Ellen Preece reports financial support, article publishing charges, statistical analysis, and writing assistance were provided by City of Stockton, Port of Stockton, California State Water Resources Control Board, Central Valley Regional Water Quality Control Board. Hans Paerl reports financial support, administrative support, equipment, drugs, or supplies, statistical analysis, travel, and writing assistance were provided by Delta Science Program, National Science Foundation, National Institute of Health.

Data availability

Data will be made available on request.

Acknowledgements

Funding for this project was provided by the City of Stockton, Port of Stockton, California Regional Water Quality Control Board Central Valley Region, and State Water Resources Control Board Freshwater Harmful Algae Bloom Program. Additional funding was provided by the National Science Foundation (projects 1831096, 1840715, 2108917 and Graduate Fellowship to HEP, 2020295001), the National Institutes of Health (1P01ES028939-01), and by an agreement with the Delta Science Program, Delta Stewardship Council (DSC contract #3885-DSC21000). Water quality analyses were conducted by Bend Genetics and Babcock Laboratories. Field assistance was provided by Central Valley Regional Water Quality Control Board's Matt Krause. We would like to thank Hailey Price for GIS work to support this project and the California Department of Water Resources Environmental Monitoring Program for loan of field equipment. We would like to thank Byran Fuhrman, Paul Bedore, Michael Bryan, and Will Hobbes for thoughtful discussions about this project and project findings. The contents may not necessarily reflect the official views or policies of the State of California.

References

- Alexander, C.A., Poulsen, F., Robinson, D.C., Ma, B.O., Luster, R.A., 2018. Improving multi-objective ecological flow management with flexible priorities and turn-taking: a case study from the Sacramento River and sacramento-san Joaquin Delta. San Franc. Estuary Watershed Sci. 16 (1).
- AOAC, 1997. Official method 972.43, microchemical determination of carbon, hydrogen, and nitrogen, automated method. In: Official Methods of Analysis of AOAC International, sixteenth ed. AOAC International, Arlington, VA, pp. 5–6 (Chapter 12)
- Bargu, S., Justic, D., White, J.R., Lane, R., Day, J., Paerl, H., Raynie, R., 2019. Mississippi River diversions and phytoplankton dynamics in deltaic Gulf of Mexico estuaries: a

- review. Estuarine. Coastal and Shelf Science 221, 39–52. https://doi.org/10.1016/j.
- Bargu, S., Skaggs, B., Boudreaux, M., Hammond, C.N., Snow, C., Aw, T.G., Stumpf, R., 2023. Water quality and toxic cyanobacteria in oligohaline estuary beaches during the longest Mississippi river basin flood event in 2019. Estuar. Coast 46, 1865–1879. https://doi.org/10.1007/s12237-023-01247-1.
- Beaulieu, J.J., DelSontro, T., Downing, J.A., 2019. Eutrophication will increase methane emissions from lakes and impoundments during the 21st century. Nat. Commun. 10, 1375. https://doi.org/10.1038/s41467-019-09100-5.
- Bergamaschi, B.A., Kraus, T.E., Downing, B.D., Soto Perez, J., O'Donnell, K., Hansen, J. A., Hansen, A.M., Gelber, A.D., Stumpner, E.B., 2020. Assessing Spatial Variability of Nutrients and Related Water Quality Constituents in the California Sacramento-San Joaquin Delta at the Landscape Scale: High Resolution Mapping Surveys. U.S. Geological Survey data release. https://doi.org/10.5066/P9FQEUAL.
- Blomqvist, P., Pettersson, A., Hyenstrand, P., 1994. Ammonium-nitrogen: a key regulatory factor causing dominance of nonnitrogen-fixing Cyanobacteria in aquatic systems. Arch. Hydrobiol. 132, 141–164.
- CCHAB Network, 2022. California HABs portal. Available from: https://mywaterquality.ca.gov/monitoring.council/cyanohab_network/.
- Chen, X., Wang, Y., Sun, T., Huang, Y., Chen, Y., Zhang, M., Ye, C., 2021. Effects of sediment dredging on nutrient release and eutrophication in the gate-controlled estuary of northern taihu lake. J. Chem. 2021, 1–13. https://doi.org/10.1155/2021/ 7451832
- Christian, R., Bryant, W., Stanley, D., 1986. The Relationship between River Flow and Microcystis Aeruginosa Blooms in the Neuse River, North Carolina. Rep. No. 223. University of North Carolina Water Resources Research Institute, Raleigh, North Carolina.
- Cornwell, J.C., Glibert, P.M., Owens, M.S., 2014. Nutrient fluxes from sediments in the San Francisco Bay Delta. Estuar. Coast 37, 1120–1133. https://doi.org/10.1007/ s12237-013-9755-4.
- Dolph, C.L., Hansen, A.T., Finlay, J.C., 2017. Flow-related dynamics in suspended algal biomass and its contribution to suspended particulate matter in an agricultural river network of the Minnesota River Basin, USA. Hydrobiologia 785, 127–147. https://doi.org/10.1007/s10750-016-2911-7.
- Erratt, K.J., Creed, I.F., Trick, C.G., 2022. Harmonizing science and management options to reduce risks of cyanobacteria. Harmful Algae 116, 102264. https://doi.org/ 10.1016/j.hal.2022.102264.
- Filippino, K.C., Egerton, T.A., Hunley, W.S., Mulholland, M.R., 2017. The influence of storms on water quality and phytoplankton dynamics in the tidal james river. Estuar. Coast 40, 80–94. https://doi.org/10.1007/s12237-016-0145-6.
- Flynn, T., Lehman, P., Lesmeister, S., Waller, S., 2022. A visual scale for Microcystis bloom severity. figshare Figure. https://doi.org/10.6084/m9.figshare.19239882.v1.
- Frantzich, J., Sommer, T., Scheier, B., 2018. Physical and biological responses to flow in a tidal freshwater slough complex. SFEWS 16. https://doi.org/10.15447/sfews.2018v16iss1/art3.
- Gao, Y., Cornwell, J.C., Stoecker, D.K., Owens, M.S., 2014. Influence of cyanobacteria blooms on sediment biogeochemistry and nutrient fluxes. Limnol. Oceanogr. 59, 959–971. https://doi.org/10.4319/lo.2014.59.3.0959.
- Glibert, P.M., 2017. Eutrophication, harmful algae and biodiversity challenging paradigms in a world of complex nutrient changes. Mar. Pollut. Bull. 124, 591–606. https://doi.org/10.1016/j.marpolbul.2017.04.027.
- Harris, D., Horwáth, W.R., Van Kessel, C., 2001. Acid fumigation of soils to remove carbonates prior to total organic carbon or CARBON-13 isotopic analysis. Soil Sci. Soc. Am. J. 65, 1853–1856.
- Huang, J., Xu, Q., Wang, X., Ji, H., Quigley, E.J., Sharbatmaleki, M., Li, S., Xi, B., Sun, B., Li, C., 2021. Effects of hydrological and climatic variables on cyanobacterial blooms in four large shallow lakes fed by the Yangtze River. Environmental Science and Ecotechnology 5, 100069, https://doi.org/10.1016/j.esc.2020.100069
- Ecotechnology 5, 100069. https://doi.org/10.1016/j.ese.2020.100069. Huisman, J., Sharples, J., Stroom, J.M., Visser, P.M., Kardinaal, W.E.A., Verspagen, J.M., Sommeijer, B., 2004. Changes in turbulent mixing shift competition for light between phytoplankton species. Ecology 85 (11), 2960–2970.
- Ibelings, B.W., Kurmayer, R., Azevedo, S.M.F.O., Wood, S.A., Chorus, I., Welker, M., 2021. Understanding the occurrence of cyanobacteria and cyanotoxins. In: Toxic Cyanobacteria in Water. CRC Press, London, pp. 213–294. https://doi.org/10.1201/ 9781003081449-4
- Jaegge, A.C., Raabe, J.M., Phillips, Z.B., Bernard, T.L., Stauffer, B.A., 2023. Flood-driven increases in phytoplankton biomass and cyanobacteria abundance in the western Atchafalaya-Vermilion Bay System, Louisiana. Hydrobiologia 850, 4413–4441. https://doi.org/10.1007/s10750-022-05029-x.
- Jassby, A.D., 2006. Phytoplankton in the upper San Francisco estuary: recent biomass trends, their causes, and their trophic significance. SFEWS 6. https://doi.org/ 10.15447/sfews.2008v6iss1art2.
- Jeffrey, S.W., Wright, S.W., Zapata, M., 1999. Recent advances in HPLC pigment analysis of phytoplankton. Mar. Freshw. Res. 50, 879–896.
- Kibuye, F.A., Zamyadi, A., Wert, E.C., 2021a. A critical review on operation and performance of source water control strategies for cyanobacterial blooms: Part Ichemical control methods. Harmful Algae 109, 102099. https://doi.org/10.1016/j. bcl.9021.102009
- Kibuye, F.A., Zamyadi, A., Wert, E.C., 2021b. A critical review on operation and performance of source water control strategies for cyanobacterial blooms: Part IImechanical and biological control methods. Harmful Algae 109, 102119. https:// doi.org/10.1016/j.hal.2021.102119.
- Kudela, R., Howard, M., Monismith, S., Paerl, H., 2023. Status, trends, and drivers of harmful algal blooms along the freshwater-to-marine gradient in the San Francisco bay-delta system. SFEWS 20. https://doi.org/10.15447/sfews.2023v20iss4art6.

- Larsen, L., Bashevkin, S., , Delta Stewardship Council, Christman, M., , Delta Stewardship Council, Conrad, J.L., 2023. California department of water resources, dahm, C., university of New Mexico, albuquerque, thompson, J., US geological survey. In: Ecosystem Services and Disservices of Bay-Delta Primary Producers: How Plants and Algae Affect Ecosystems and Respond to Management of the Estuary and its Watershed. SFEWS 20. https://doi.org/10.15447/sfews.2023v20iss4art1.
- Laureano-Rosario, A.E., McFarland, M., Bradshaw, D.J., Metz, J., Brewton, R.A., Pitts, T., Perricone, C., Schreiber, S., Stockley, N., Wang, G., Guzmán, E.A., Lapointe, B.E., Wright, A.E., Jacoby, C.A., Twardowski, M.S., 2021. Dynamics of microcystins and saxitoxin in the Indian River Lagoon, Florida. Harmful Algae 103, 102012. https://doi.org/10.1016/j.hal.2021.102012.
- Lehman, P.W., Marr, K., Boyer, G.L., Acuna, S., Teh, S.J., 2013. Long-term trends and causal factors associated with Microcystis abundance and toxicity in San Francisco Estuary and implications for climate change impacts. Hydrobiologia 718, 141–158. https://doi.org/10.1007/s10750-013-1612-8.
- Lehman, P.W., Kendall, C., Guerin, M.A., Young, M.B., Silva, S.R., Boyer, G.L., Teh, S.J., 2015. Characterization of the Microcystis bloom and its nitrogen supply in San Francisco estuary using stable isotopes. Estuar. Coast 38, 165–178. https://doi.org/ 10.1007/s12237-014-9811-8.
- Lehman, P.W., Kurobe, T., Lesmeister, S., Baxa, D., Tung, A., Teh, S.J., 2017. Impacts of the 2014 severe drought on the Microcystis bloom in San Francisco Estuary. Harmful Algae 63, 94–108. https://doi.org/10.1016/j.hal.2017.01.011.
- Lehman, P.W., Kurobe, T., Teh, S.J., 2022. Impact of extreme wet and dry years on the persistence of Microcystis harmful algal blooms in San Francisco Estuary. Quat. Int. 621, 16–25. https://doi.org/10.1016/j.quaint.2019.12.003.
- Likens, G.E., 1972. Nutrients and eutrophication. In: Spec. Symp. 1, American Society of Limnology and Oceanography. Allen Press.
- Liu, X., Li, Y.-L., Liu, B.-G., Qian, K.-M., Chen, Y.-W., Gao, J.-F., 2016. Cyanobacteria in the complex river-connected Poyang Lake: horizontal distribution and transport. Hydrobiologia 768, 95–110. https://doi.org/10.1007/s10750-015-2536-2.
- Lund, J., 2016. California's agricultural and urban water supply reliability and the sacramento-san Joaquin Delta. SFEWS 14. https://doi.org/10.15447/ sfews.2016v14iss3art6.
- Luoma, S.N., Dahm, C.N., Healey, M., Moore, J.N., 2015. Water and the sacramento-san Joaquin Delta: complex, chaotic, or simply cantankerous? SFEWS 13. https://doi. org/10.15447/sfews.2015v13iss3art7.
- Lürling, M., Van Oosterhout, F., Faassen, E., 2017. Eutrophication and warming boost cyanobacterial biomass and microcystins. Toxins 9, 64. https://doi.org/10.3390/ toxins0020064
- Ma, L., Moradinejad, S., Guerra Maldonado, J.F., Zamyadi, A., Dorner, S., Prévost, M., 2022. Factors affecting the interpretation of online phycocyanin fluorescence to manage cyanobacteria in drinking water sources. Water 14, 3749. https://doi.org/ 10.3200/w1403740
- Moss, B., 2011. Allied attack: climate change and eutrophication. IW 1 101–105. https://doi.org/10.5268/IW-1.2.359.
- Newell, S.E., Davis, T.W., Johengen, T.H., Gossiaux, D., Burtner, A., Palladino, D., McCarthy, M.J., 2019. Reduced forms of nitrogen are a driver of non-nitrogen-fixing harmful cyanobacterial blooms and toxicity in Lake Erie. Harmful Algae 81, 86–93.
- Oksanen, J., Simpson, G., Blanchet, F., Kindt, R., Legendre, P., Minchin, P., O'Hara, R., Solymos, P., Stevens, M., Szoecs, E., Wagner, H., Barbour, M., Bedward, M., Bolker, B., Borcard, D., Carvalho, G., Chirico, M., De Caceres, M., Durand, S., Evangelista, H., FitzJohn, R., Friendly, M., Furneaux, B., Hannigan, G., Hill, M., Lahti, L., McGlinn, D., Ouellette, M., Ribeiro Cunha, E., Smith, T., Stier, A., Ter Braak, C., Weedon, J., 2022. Vegan: community ecology package. R package version 2.6-4. https://CRAN.R-project.org/package=vegan.
- Paerl, H.W., 2014. Mitigating harmful cyanobacterial blooms in a human- and climatically-impacted world. Life. https://doi.org/10.3390/life40x000x.
- Paerl, H.W., 2023. Climate change, phytoplankton, and HABs. In: Kennish, M., Paerl, H., Crosswell, J. (Eds.), Climate Change and Estuaries. CRC Press, pp. 315–334.
- Paerl, H.W., Huisman, J., 2008. Blooms like it hot. Science 320 (5872), 57–58.
 Paerl, H.W., Huisman, J., 2009. Climate change: a catalyst for global expansion of harmful cyanobacterial blooms. Environ. Microbiol. Rep. 1 (1), 27-3.
- Paerl, H.W., Otten, T.G., Kudela, R., 2018. Mitigating the expansion of harmful algal blooms across the freshwater-to-marine continuum. Environ. Sci. Technol. 52,
- 5519–5529. https://doi.org/10.1021/acs.est.7b05950.
 Phlips, E.J., Badylak, S., Mathews, A.L., Milbrandt, E.C., Montefiore, L.R., Morrison, E.S., Nelson, N., Stelling, B., 2023. Algal blooms in a river-dominated estuary and nearshore region of Florida, USA: the influence of regulated discharges from water control structures on hydrologic and nutrient conditions. Hydrobiologia 850, 4385–4411. https://doi.org/10.1007/s10750-022-05135-w.
- Preece, E.P., Hardy, F.J., Moore, B.C., Bryan, M., 2017. A review of microcystin detections in Estuarine and Marine waters: environmental implications and human health risk. Harmful Algae 61, 31–45. https://doi.org/10.1016/j.hal.2016.11.006.
- PSEP, 1997. Recommended Guidelines for Sampling Marine Sediment, Water Column, and Tissue in Puget Sound. Prepared for U.S. Environmental Protection Agency Region 10, Seattle, WA and Puget Sound Water Quality Authority, Olympia, WA by King County.
- Qin, B., Zhou, J., Elser, J.J., Gardner, W.S., Deng, J., Brookes, J.D., 2020. Water depth underpins the relative roles and fates of nitrogen and phosphorus in lakes. Environ. Sci. Technol. 54, 3191–3198. https://doi.org/10.1021/acs.est.9b05858.

- Rahutomo, S., Kovar, J.L., Thompson, M.L., 2018. Varying redox potential affects P release from stream bank sediments. PLoS One 13, e0209208. https://doi.org/ 10.1371/journal.pone.0209208.
- Robson, B.J., Hamilton, D.P., 2004. Three-dimensional modelling of a Microcystis bloom event in the swan River estuary, western Australia. Ecol. Model. 174, 203–222. https://doi.org/10.1016/j.ecolmodel.2004.01.006.
- Saleh, D., Domagalski, J., 2021. Concentrations, loads, and associated trends of nutrients entering the sacramento-san Joaquin Delta, California. SFEWS 19. https://doi.org/ 10.15447/sfews.2021v19iss4art6.
- Sandrini, G., Ji, X., Verspagen, J.M.H., Tann, R.P., Slot, P.C., Luimstra, V.M., Schuurmans, J.M., Matthijs, H.C.P., Huisman, J., 2016. Rapid adaptation of harmful cyanobacteria to rising CO₂. Proc. Natl. Acad. Sci. U.S.A. 113, 9315–9320. https:// doi.org/10.1073/pnas.1602435113.
- Schladow, S.G., Monismith, S., 2009. Hydrodynamics and oxygen modeling of the Stockton deep water ship channel. In: Final Report for CALFED ERP-02d-P51.
- Sepulveda-Jauregui, A., Hoyos-Santillan, J., Martinez-Cruz, K., Walter Anthony, K.M., Casper, P., Belmonte-Izquierdo, Y., Thalasso, F., 2018. Eutrophication exacerbates the impact of climate warming on lake methane emission. Sci. Total Environ. 636, 411–419. https://doi.org/10.1016/j.scitotenv.2018.04.283.
- Smith, V.H., 2003. Eutrophication of freshwater and marine ecosystems: a global problem. Environ. Sci. Pollut. Res. Int. 10, 126–139.
- Spier, C., Stringfellow, W., Hanlong, J., Brunell, M., Estiandan, M., Koski, T., Kääriä, 2013. Unprecedented Bloom of Toxin-Producing Cyanobacteria in the Southern Bay-Delta Estuary and its Potential Negative Impact on the Aquatic Food Web. University of the Pacific Ecological Engineering Research Program. Report 4.5.1. December.
- Ta, J., Anderson, L., Christman, M., Khanna, S., Kratville, D., Madsen, J., Moran, P., Viers, J., 2017. Invasive aquatic vegetation management in the sacramento-san Joaquin River Delta: status and recommendations. SFEWS 15. https://doi.org/10.15447/sfews.2017v15iss4art5.
- Tett, P., Gilpin, L., Svendsen, H., Erlandsson, C.P., Larsson, U., Kratzer, S., Fouilland, E., Janzen, C., Lee, J.-Y., Grenz, C., Newton, A., Ferreira, J.G., Fernandes, T., Scory, S., 2003. Eutrophication and some European waters of restricted exchange. Continent. Shelf Res. 23, 1635–1671. https://doi.org/10.1016/j.csr.2003.06.013.
- Vaičiūtė, D., Bučas, M., Bresciani, M., Dabulevičienė, T., Gintauskas, J., Mėžinė, J., Tiškus, E., Umgiesser, G., Morkūnas, J., De Santi, F., Bartoli, M., 2021. Hot moments and hotspots of cyanobacteria hyperblooms in the Curonian Lagoon (SE Baltic Sea) revealed via remote sensing-based retrospective analysis. Sci. Total Environ. 769, 145053 https://doi.org/10.1016/j.scitotenv.2021.145053.
- Verspagen, J., 2006. Benthis-pelagic coupling in the population dynamics of the cyanobacterium Microcystis = Benthisch-pelagische koppeling in de populatie dynamica van de cyanobacterie Microcystis (s.n., S.l).
- Visser, P.M., Verspagen, J.M.H., Sandrini, G., Stal, L.J., Matthijs, H.C.P., Davis, T.W., Paerl, H.W., Huisman, J., 2016. How rising CO2 and global warming may stimulate harmful cyanobacterial blooms. Harmful Algae 54, 145–159. https://doi.org/ 10.1016/i.hal.2015.12.006.
- Walve, J., Sandberg, M., Elmgren, R., Lännergren, C., Larsson, U., 2021. Effects of load reductions on phosphorus concentrations in a baltic estuary—long-term changes, seasonal variation, and management implications. Estuar. Coast 44, 30–43. https:// doi.org/10.1007/s12237-020-00769-2.
- Wang, Q., Li, Y., 2010. Phosphorus adsorption and desorption behavior on sediments of different origins. J. Soils Sediments 10, 1159–1173. https://doi.org/10.1007/ s11368-010-0211-9.
- Wang, J., Zhang, Z., 2020. Phytoplankton, dissolved oxygen and nutrient patterns along a eutrophic river-estuary continuum: observation and modeling. J. Environ. Manag. 261, 110233 https://doi.org/10.1016/j.jenvman.2020.110233.
- Wilkerson, F.P., Dugdale, R.C., Hogue, V.E., Marchi, A., 2006. Phytoplankton blooms and nitrogen productivity in San Francisco Bay. Estuar. Coast 29, 401–416. https://doi. org/10.1007/BF02784989.
- Xu, H., McCarthy, M.J., Paerl, H.W., Brookes, J.D., Zhu, G., Hall, N.S., Qin, B., Zhang, Y., Zhu, M., Hampel, J.J., Newell, S.E., Gardner, W.S., 2021. Contributions of external nutrient loading and internal cycling to cyanobacterial bloom dynamics in Lake Taihu, China: implications for nutrient management. Limnol. Oceanogr. 66, 1492–1509. https://doi.org/10.1002/lno.11700.
- Yang, J., Tang, H., Zhang, X., Zhu, X., Huang, Y., Yang, Z., 2018. High temperature and pH favor Microcystis aeruginosa to outcompete Scenedesmus obliquus. Environ. Sci. Pollut. Res. 25, 4794–4802. https://doi.org/10.1007/s11356-017-0887-0.
- You, J., Mallery, K., Hong, J., Hondzo, M., 2018. Temperature effects on growth and buoyancy of Microcystis aeruginosa. J. Plankton Res. 40, 16–28. https://doi.org/ 10.1093/plankt/fbx059.
- Zepernick, B.N., Gann, E.R., Martin, R.M., Pound, H.L., Krausfeldt, L.E., Chaffin, J.D., Wilhelm, S.W., 2021. Elevated pH conditions associated with Microcystis spp. blooms decrease viability of the cultured diatom fragilaria crotonensis and natural diatoms in lake erie. Front. Microbiol. 12, 598736 https://doi.org/10.3389/fmicb.2021.598736.
- Zepernick, B.N., Wilhelm, S.W., Bullerjahn, G.S., Paerl, H.W., 2023. Climate change and the aquatic continuum: a cyanobacterial comeback story. Environ Microbiol Rep 15, 3–12. https://doi.org/10.1111/1758-2229.13122.